Article

Photometric analysis and light curve modeling of apparent transient 2020pni

Hemal Arora[1], Arya Maheshwari[2], Audrey O'Malley[3], Jason Wu[4], Michael Warrener[5], Michael Faison[5]

[1] United World College of South East Asia, 1 Tampines Street 73, Singapore 528704
[2] The Harker School, 500 Saratoga Avenue, San Jose, CA 95129, USA
[3] Plano Senior High School, 2200 Independence Pkwy, Plano, TX 75075, USA
[4] Shady Side Academy, 423 Fox Chapel Rd., Pittsburgh, PA 15238, US
[5] Yale University, Steinbach Hall, 52 Hillhouse Avenue, New Haven, CT 06511

SUMMARY

By meticulously observing and analyzing the characteristics of individual cosmic events, we are better suited to understand the universe on a broader scale. Specifically, astronomers are often drawn to examine transient astronomical events whose duration may range from days to several years. This relatively short timescale, in contrast to the billions of years over which our universe has evolved, makes these events highly valuable as snapshots of how our universe is shaped. Spurred by this prospect, our team searched catalogues of these transient astronomical events and decided to investigate apparent transient 2020pni from galaxy UGC 9684. We hypothesized that the transient was a supernova—a powerful stellar explosion caused by the gravitational collapse of a massive star. Thus, we observed the transient over a four-week period to test this hypothesis by measuring changes in the intensity of light radiated by the event—a process known as photometric analysis. Through this study, our team was able to confirm our hypothesis and classify 2020pni as a Type II-L supernova. In addition, we unraveled key insights about the supernova's distance from Earth, stellar composition, luminosity, and more.

INTRODUCTION

A transient astronomical event is an astronomical phenomenon with a relatively short time scale, ranging from several years to even weeks and days. Often, these transients are deep-space events, such as supernovae, dwarf novae, and gamma-ray bursts.

Our team had several key motivations for specifically investigating supernovae in this study. For instance, supernovae are used as standard candles, or celestial objects with a known intrinsic brightness, for measuring cosmic distances throughout the universe. By finding the apparent magnitudes of supernovae and matching them with their theoretical absolute magnitudes, a distance modulus can be used to find their distances from Earth. Thus, the study of supernovae aids in illustrating a broader picture of the universe's structure. Besides, supernovae are an essential factor in perpetuating stellar evolution throughout

our universe. Heavy elements produced by these explosions enrich stars and planets alike, contributing to celestial bodies with exotic physical properties. Furthermore, the current method by which supernovae are classified, established in 1941 by American astronomers Rudolph Minkowski and Fritz Zwicky, is becoming dated and, therefore, requires as much data as possible to modernize and update it (1). By inspecting a large number of supernovae, we actively improve the method with which they are studied. In addition, this allows us to build on the body of knowledge on the various types of supernovae. These include Type I-a (explosions of binary star systems which include a white dwarf), Type I-b (which involves the core collapse of massive stars) and Type II (which result from the collapse of a star 8 to 40 times the mass of the sun). Type II supernovae are also sub-divided into Type II-L (linear) and II-P (plateau) as some demonstrate a linear decrease in brightness over time while others have a plateau in brightness before fading away.

In July of 2020, our team read about the discovery of the apparent transient (AT) 2020pni (2). At the time, it was listed as an early supernova candidate, hosted by galaxy UGC 9684. When a star undergoes a supernova explosion, it violently shreds its stellar atmosphere, producing an outburst of light luminous enough to be seen thousands of lightyears away. Initial reports had indicated that the transient's luminosity increased by 1.8 magnitudes shortly after discovery— unusual for an otherwise stable galaxy like UGC 9684. The reports had also pinpointed hydrogen (H) and helium (He) lines in the transient's spectrum, a characteristic feature for Type II supernovae (1). It is for these reasons that our team hypothesized AT2020pni is a supernova.

To test our hypothesis, our team observed the transient over a four-week period with the telescopes at the Leitner Family Observatory and Planetarium (LFOP) at Yale University and the iTelescope network (3). During this time, we captured the target in different light filters for the sake of photometry—the process of measuring the intensity of light radiating from astronomical objects—and color corrections. This process was used to convert our brightness measurements to instrumental and calibrated magnitudes which, when plotted over time, yield a light curve— a graph depicting the brightness of an object over a period of time. If

the transient's light curve fits well with standard supernova light curve models, our team could confirm the supernova and gain key insights regarding the event's chemical composition, mass, distance, and temperature.

Through our work, we classified AT2020pni as a Type II-L supernova, estimated it to lie 47.9 megaparsec (Mpc) away from Earth and deduced that it had a peak luminosity approximately 8.39×10^8 times the luminosity of the sun.

RESULTS

AT2020pni is in the host galaxy UGC 9684 and has a right ascension of 15h 03m 49.964s and a declination of +42° 06' 50.52" (J2000 coordinates) as discovered on 2020/07/16 (2). Upon observing these coordinates, we found that Supernova AT2020pni is clearly distinguishable from, despite being in close proximity to, its host galaxy (**Figure 1**). This made it ideal for our study.

The following results are based on our data collection while observing the target through Charge-Coupled Device (CCD) images taken with a 0.50-meter f/6.8 telescope from the iTelescope network and 16-inch Richtey-Chretien f/8.9 telescope at Yale University. To observe the transient, we utilized two sets of color filters, which isolate light with wavelengths in a specific region around a central wavelength: Johnson V and R, which have central wavelengths of 366 and 435 nm respectively, and Sloan g and r filters, which have central wavelengths of 477 and 623 nm respectively. We used the measurements from each observation to calculate the transient's flux and, through calculations involving standard stars in the field of view with known magnitudes (brightnesses), we converted the transient's flux to a standard magnitude.

Calibrated magnitudes in two colors

To test our hypothesis that transient AT2020pni is a supernova, we first obtained calibrated magnitudes for the supernova at various times in two colors. We catalogued these apparent V and R magnitudes for each day of observation, as determined from our aperture photometry pipeline and subsequent color calibration based on standard stars (**Table 1**). Our results demonstrated a general decreasing trend in the apparent brightness of AT2020pni (**Figure 2**).

Light curve fitting

We next utilized our calibrated magnitude measurements and fitted them with standard supernova light curves, which are plots of an object's brightness over time. Apparent magnitudes of AT2020pni were fitted to four standard light curve models for supernovae (**Figure 3**). The fit was promising, as our observations of AT2020pni matched well with the characteristic variation in intensity for supernovae. Specifically, our observations fit exceptionally well with the standard light curve of a Type II-L supernova with a relatively low root-mean-squared error (RMSE) of 0.1283 (**Table 2**). Thus, we confirmed our hypothesis that AT2020pni is a
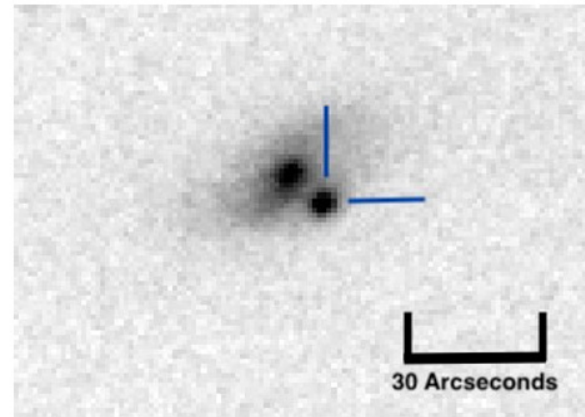

Figure 1. A Charge-Coupled Device (CCD) image of Apparent Transient AT2020pni. AT2020pni is marked with blue lines and distinguishable from its host galaxy UGC 9684. The brightness of the transient is comparable to that of its entire host galaxy.
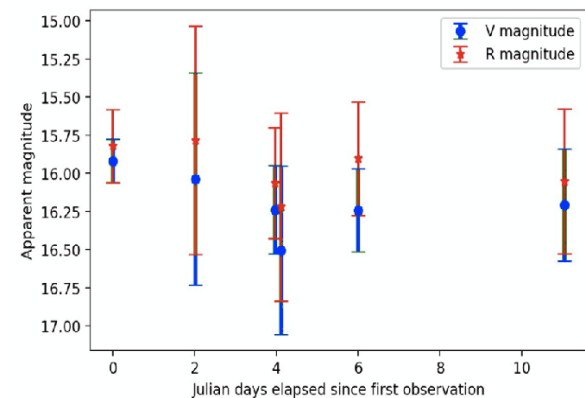

Figure 2. The Calibrated Magnitudes for AT2020pni in Two Colors. The apparent magnitudes recorded for AT2020pni in the V and R filters (isolating distinct wavelength regions) plotted against time.
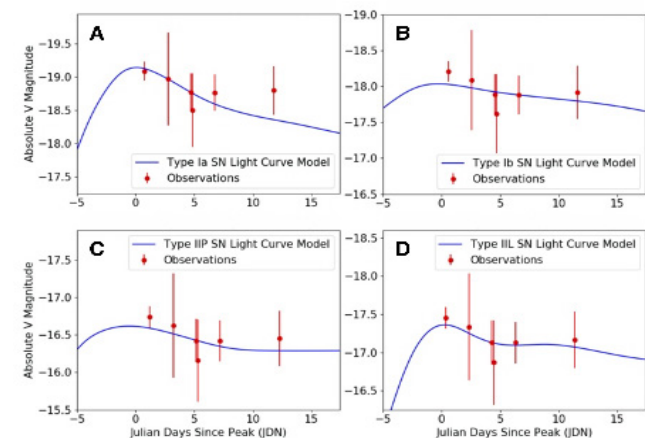

Figure 3. Apparent Magnitudes for AT2020pni Fitted to Standard Supernova Light Curves. Our apparent magnitude data for AT2020pni was fitted to standard light curve models of four supernova types to determine which classification best models the event. The supernova types tested include A) Type I-a (explosions of binary star systems which include a white dwarf), B) Type I-b (which involves the core collapse of massive stars) and C) Type II-P and D) II-L (which both result from the collapse of a star 8 to 40 times the mass of the sun).

supernova and further concluded that it is a Type II-L (II-Linear) which should demonstrate a rapid, linear decay from its peak brightness.

We then plotted the absolute V magnitude light curve of supernova 2020pni over the theoretical model of a Type II-L supernova (**Figure 4**). The x-axis is the Julian Day Number (a standardized astronomical method of marking the date and time of a measurement) of our observations since the peak brightness of the model. On the y-axis, our calculated apparent V magnitudes were shifted to best-fit absolute magnitudes. That said, Type II-L supernovae are not standard candles, meaning that they do not have a known and consistent absolute magnitude. As such, the absolute magnitudes calculated by shifting the apparent V magnitudes upwards are an approximation.

While the RMSE of our data for AT2020pni is lowest for a type II-L supernova, a longer observation period of several more weeks could strengthen this claim.

Color index curve

An additional insight that can be derived from our apparent magnitudes is an understanding of the temperature variation of the supernova from a color index curve. It was useful to plot a color index curve of apparent (V-R) vs. time (**Figure 5**). The color values seem to decrease slightly over time, only suggesting a slight amount of reddening and cooling of the supernova, if any, over the course of our observations. To identify a more distinct trend, a wider range of observation times of several more weeks would have been necessary, especially given the large uncertainties.

Distance and luminosity estimates

Finally, our team sought to investigate the distance and luminosity of the supernova with our data. It should be noted that Type II-L supernovae are not true standard candles like Type Ia supernovae (supernovae which occur in binary star systems containing a white dwarf). Despite this, the vertical shift between our data and the standard absolute magnitude models can still be used as an approximate distance modulus to make a rough estimate of the distance between the supernova and Earth. Thus, using **Equation 5**, an approximate distance modulus of 33.4, calculated from our optimal model fit, yielded a distance estimate of 47.9 megaparsec (Mpc).

We compared our distance estimate of 47.9 Mpc with the distance that would be calculated using **Equation 6**, which is Hubble's law. Hubble's law linearly relates the distance to an object and its recession velocity. The velocity of the host galaxy, which we assumed as a proxy for the supernova given their effectively equal distances, was derived from its redshift. Redshift is a quantity often reported in astronomical data sets which is related to an object's velocity and the speed of light. Using the host galaxy's redshift of $z = 0.01687$ stated in the discovery report for AT2020pni, this method results in a distance of 72.3 Mpc (2). Therefore, the light curve

Date, JDN	Filter	App. Mag.	Error
07/25/20	V	15.9	0.1
2459056.60	R	15.8	0.2
07/27/20	V	16.0	0.7
2459058.61	R	15.8	0.7
07/29/20	V	16.2	0.3
2459060.57	R	16.1	0.4
07/29/20	V	16.5	0.3
2459060.71	R	16.4	0.4
07/31/20	V	16.2	0.4
2459062.60	R	15.9	0.5
08/05/20	V	16.2	0.6
2459067.64	R	16.1	0.6

Table 1. Apparent magnitude (App. Mag.) values recorded for AT2020pni over each day of observation (provided in Julian Day Number (JDN) format) for both the V and R filters.

Model Type	Ia	Ib	**II-L**	II-P
RMSE	0.2406	0.1613	**0.1283**	0.1636

Table 2. RMSE values for fitting AT2020pni V-filter apparent magnitudes to standard light curve models. The best-fit model for AT2020pni is Type II-L.

based distance measurement was consistent as an order-of-magnitude estimate with the redshift-based distance. The factor-of-two difference was likely caused by our treatment of Type II-L supernovae as standard candles for estimation purposes in this calculation.

We used the absolute magnitude to understand the intrinsic luminosity or brightness of the supernova as well. Using the accepted value of $M_{Sun} = 4.83$ in Equation 7, the peak luminosity of AT2020pni is derived to be approximately 8.39×10^8 $L_\odot$, based on a peak absolute magnitude of $L_{SN} = -17.5$. This makes AT2020pni one of the brighter supernovae of its type, as Type II supernovae average around an absolute magnitude of -18.6 (4).

DISCUSSION

The study of supernovae helps us understand the processes that perpetuate the evolution of our universe.

Thus, due to our interest in contributing to the body of knowledge on supernovae, our team sought to find an early supernova candidate and investigate it. Having read about AT2020pni—a recent transient astronomical event—our team hypothesized that the transient was, in fact, a supernova and observed it over a four-week period. Through this process, we confirmed our hypothesis and produced insights ranging from the supernova's approximate distance from Earth to its temperature variation.

We concluded in this study that AT2020pni is a Type II-L supernova based on photometric data taken over multiple days, which fit standard models of supernova light curves. This result supported our hypothesized classification of AT2020pni as a supernova due to its rapid increase in luminosity and preliminary findings of H and He II emission lines found in the 400-800 nm range of the transient's light spectrum. As these emission lines can be exhibited by Type II supernovae, our work served as an independent validation of these preliminary findings in the transient's discovery reports (2).

Our classification predicts that AT2020pni will continue to evolve with a linear decrease in brightness, rather than the plateau characteristic of Type II-P (II-Plateau) supernovae. While Type II-L supernovae are still hydrogen rich, the linear decay suggests intriguing physical processes that are distinct from the electron recombination that causes the plateau in the brightness of Type II-P supernovae (5). It is possible that the AT2020pni progenitor had a thinner hydrogen shell, leading to less recombination during the explosion. Alternatively, there may have been a disruptive event that inflated the peak brightness of the supernova earlier on (5).

We derived a number of additional physical insights regarding AT2020pni by fitting our measurements to theoretical models for Type II-L supernovae. Our data suggested a peak absolute magnitude of approximately -17.5 on 07/25/20 (our first day of observation) and a corresponding peak luminosity of 8. By treating the vertical offset required to fit the II-L model as a rough distance modulus, we estimated the distance to AT2020pni to be approximately 47.9 Mpc, which is consistent within an order-of-magnitude with a z = 0.01687 redshift-based distance calculation of 72.3 Mpc.

Continued observation of AT2020pni, spanning over several more weeks, would help strengthen current conclusions on the supernova's type, based on the contrasting dimming rates for different types of supernovae. Additionally, AT2020pni's brightness made it a potential candidate for spectroscopy given a long enough exposure time and optimal viewing conditions. However, telescopes with greater sensitivities than the ones used in this study would likely be required. New spectroscopic measurements could lead to a quantitative and specific understanding of the supernova's composition and physical properties. Additionally, it would be fascinating to investigate P-Cygni profiles in the spectrum, where the presence of both absorption and emission in the profile of a spectral line indicates the existence of a gaseous
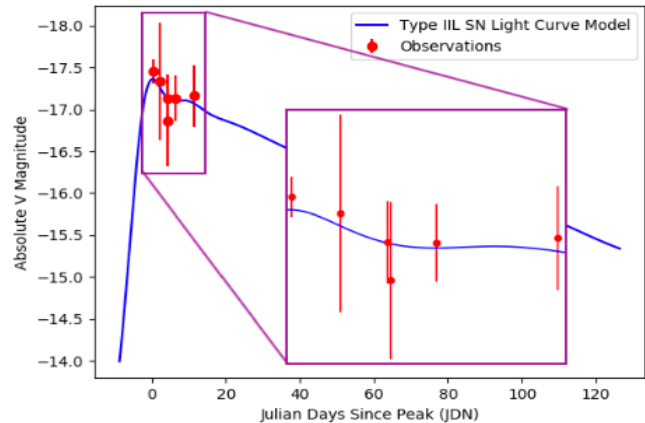

Figure 4. Absolute V Magnitudes of AT2020pni over a Type II-L Supernova Light Curve The absolute V magnitude light curve of supernova AT2020pni, plotted over the theoretical model of a Type II-L supernova. The x-axis is the Julian Day Number (a standardized astronomical method of recording time) of our observations since the peak brightness of the model. The calculated apparent V magnitudes were shifted to best-fit absolute magnitudes on the y-axis. The boxed zoom provides a more detailed view of each data point.
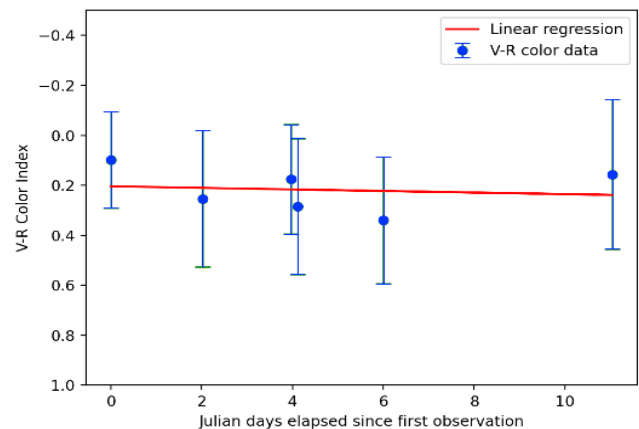

Figure 5. A Color Index Curve of AT2020pni. The color index curve of the apparent V-R magnitudes of AT2020pni plotted against time. This provides insight into the temperature variation of the supernova over time. The downward sloping linear regression indicates a slight amount of cooling of the supernova.

envelope expanding away from the star (5).

Finally, given the proximity and partial overlap of AT2020pni with its host galaxy, a possible improvement to the aperture photometry methods used in our study could be point-spread-function (PSF) photometry (6). PSF photometry is especially useful for isolating light from sources in crowded fields and could, thus, help better differentiate the supernova's light from the host galaxy's, which is crucial for accurately determining the magnitude of the supernova.

Overall, our photometric study of AT2020pni deepened our understanding of this recent transient astronomical event. We confirmed our hypothesis that AT2020pni is an extragalactic supernova and classified it as Type II-L, adding to the body of knowledge about all supernovae of this type.

Additionally, by correlating our observations with absolute magnitudes of standard Type II-L supernovae, we estimated peak magnitude, luminosity, distance, and temperature trends for this supernova, all of which provided additional observational insights regarding Type II-L supernovae and helped broaden our understanding of the physics of stellar evolution.

MATERIALS AND METHODS
Data Collection

In order to collect data on our observing target, we captured CCD images of the transient and the surrounding region of sky. We utilized two telescopes for observations: A 16-inch Ritchey-Chretien telescope (f/8.9) at the LFOP at Yale University and the iTelescope network's 0.50 meter (f/6.8) T11 telescope at its New Mexico Skies Observatory. A SBIG STL-1001E CCD Camera and FLI ProLine PL11002M CCD camera were connected to the 16-inch telescope and T11 respectively (7). Observing sessions on both telescopes were done using automated queue observing.

Photometric color calibration requires data from two separate colors, so images were taken in two filters: the Johnson V and R filters for T11 and the Sloan g and r filters for the 16-inch telescope (7) (8). While the brightness measured through these filters may vary slightly, given the similar wavelength regimes of the corresponding filters, we expected that these differences would be marginal. Nevertheless, through color calibration procedures using a linear transformation from instrumental to absolute magnitudes, we standardized our measurements in both filters to the Sloan system. As such, we use 'V' to refer to both Johnson V and Sloan g, and 'R' to refer to both Johnson R and Sloan r, unless stated otherwise.

A summary of our observing sessions is listed in **Table S1**. Data was successfully obtained six times over the course of 10 days, a period of time that, while not spanning a large portion of the supernova's full light curve, should generate noticeable differences between the different supernova types. All observations were done with 1x1 binning—meaning that measurements from individual pixels were not binned together—to optimize for resolution over sensitivity in order to best distinguish AT2020pni from its host galaxy.

Data Processing and Photometric Analysis

Collected images from observation sessions were processed using the image processing software MaxIm DL (9). The images for each filter were flat-fielded and median combined with bicubic resampling and automatic star matching enabled, which are standard image preprocessing techniques to remove variations across pixels and across images. Through this process, the signal-to-noise ratios of the combined images of the V and R filters were increased by a factor of the square root of the number of sub-exposures since signal increases linearly and noise increases with the square root of the number of sub-exposures. Additionally, the
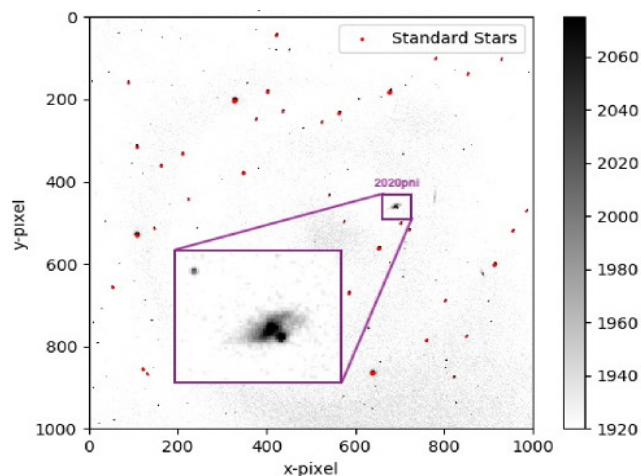

Figure 6. A CCD image of Standard Stars Around AT2020pni. Standard stars in the field of view of AT2020pni acquired from the Pan-STARRS1 sky survey along with a zoomed-in image of AT2020pni itself.

combined images for V and R were aligned with each other using automatic star matching.

To conduct VR photometry using our data, we used standard magnitudes of standard stars in the field of view of our images as reference apparent magnitudes with which to calibrate the apparent magnitude of AT2020pni. A table of the right ascensions, declinations, and Sloan g and r standard magnitudes of standard stars was acquired from the Pan-STARRS1 sky survey via the VizieR catalog service (10). We omitted stars with magnitudes dimmer than 17 or with large photometric errors (greater than 0.1 magnitude) to improve the precision of our analysis.

In order to map these standard stars from their celestial coordinates to pixel locations in the CCD images, we acquired World Coordinate System (WCS) files and plate-solved our images using Astrometry.net. Standard stars located in the field of view of our image data are shown in **Figure 6**, along with the location of AT2020pni.

Using Photutils, an Astropy package for detection and photometry of astronomical sources, we programmed an aperture photometry tool to extract the instrumental magnitudes of the standard stars from our images in the V and R filters for each day. The program added all the pixel values in a 6-pixel-radius circular aperture around the location of each standard star. It then subtracted an average local background based on an annulus with an inner radius of 10 pixels and an outer radius of 12 pixels (**Figure S1**). The resulting values were the electron-counts (or fluxes) of our standard stars.

The instrumental magnitude was calculated from the electron count using **Equation 1**, a statement of the logarithmic scale for instrumental magnitude, where m is the instrumental magnitude and b is the flux in electron counts measured by the photometry tool.

$$m = -2.5log(b) \qquad (1)$$

By repeating this process for all standard stars in the combined images of both filters, the instrumental magnitudes (denoted with v and r) and standard magnitudes (denoted with V and R) of various standard stars were obtained in order to build models for color calibration. By performing two least-squares regressions based on the BVR photometry transformation equations (**Equations 2** and **3**) shown below, we obtained the regression coefficients T_{vr}, C_{vr}, T_V and C_V which will be used to calibrate our supernova's instrumental magnitude. An example of such a regression is shown in **Figure S2**.

$$V - R = T_{vr}(v - r) + C_{vr} \qquad (2)$$

$$V = v + T_V(V - R) + C_V \qquad (3)$$

The supernova's flux was measured with aperture photometry at the pixel location of the supernova, using a circular aperture radius of 5 pixels and inner and outer annular radii of 5 and 10 pixels, respectively. After obtaining a resultant instrumental magnitude with **Equation 1**, the transformation coefficients from **Equations 2** and **3** were used to calculate the standard apparent V and R magnitudes for the supernova. This photometric analysis pipeline was repeated for every observation day's data set.

Light curve and color curve plots

A light curve is a graph of the light intensity (measured as the absolute magnitude) of a celestial object over time. The measurements of the transient's calibrated apparent magnitudes from the photometric analysis section were paired with the Julian Day Number corresponding to the time of observation. These data were fitted to four different light curve models of the typical absolute magnitude fluctuations of various supernovae types (Type Ia, Type Ib, Type II-L, and Type II-P) to determine the best fit. We utilized a gradient descent algorithm to optimize the offsets by which to shift the apparent magnitudes upwards and along the x-axis to minimize the RMSE between our observational data on a certain day and the absolute magnitude predicted by the light curve model at that x-value. The model light curve with the lowest RMSE was used to classify the transient, as well as to derive additional properties, such as its approximate distance and peak luminosity.

Furthermore, the difference of the V and R magnitudes is used to quantitatively assess the color of our target. The resulting color index is then plotted against time of observation to form a color index curve, which could offer further insights into the mechanism and surrounding conditions of the supernova.

Uncertainty Analysis

Uncertainties in measured apparent magnitudes were derived from the uncertainty of the linear regressions used in the color calibration and offset linear transforms. For

apparent V magnitudes, the uncertainties (error bar sizes) were determined to be ±2 × RMSE of the linear fit generated by **Equation 3**. Assuming a Gaussian distribution of possible values above and below each point on the line, 95% of the values would fall in the range of this uncertainty. For apparent R magnitudes, the RMSE values of **Equations 2** and **3** were combined by adding each individual RMSE in quadrature, as in **Equation 4**.

$$\text{Unc}_R = \pm 2 \cdot {}^2\sqrt{(\text{RMSE}_2)^2 + (\text{RMSE}_3)^2} \qquad (4)$$

Slopes and intercepts of the linear regression for each observing session are compiled in **Table S2**, which shows how values of T_{vr} approach 1 while C_{vr} and T_V approach 0.

Additional Equations

In addition to those mentioned above, we utilized the following equations to analyze the processed data we collected.

Equation 5 describes the distance modulus we used to estimate the distance between Earth and the supernova. In the equation, m is the apparent V magnitude, M is the absolute V magnitude from the light curve (m-M is the distance modulus), and d is the distance between Earth and the supernova in parsecs.

$$m - M = 5\log(d) - 5 \implies d = 10^{\frac{m-M+5}{5}} \qquad (5)$$

Equation 6 is Hubble's law, where H_0 is the Hubble constant, d is the distance between Earth and the supernova, v is the velocity of the host galaxy, z is the redshift of the host galaxy, and c is the speed of light.

$$H_0 d = v = zc \implies d = \frac{zc}{H_0} \qquad (6)$$

Equation 7 relates the difference in absolute magnitudes between the Sun and the supernova to the ratio of their intrinsic luminosities. In the equation, M_{SN} and L_{SN} are the magnitude and luminosity of the supernova, and M_{Sun} and $L_\odot$ are the solar magnitude and luminosity, respectively.

$$M_{SN} = M_{Sun} = -2.5\log\left(\frac{L_{SN}}{L_\odot}\right) \qquad (7)$$

REFERENCES

1. Da Silva, L. A. "The Classification of Supernovae." Astrophysics and Space Science, vol. 202, no. 2, 1993, doi:10.1007/bf00626878.
2. Bruch, Rachel. "AstroNote 2020-136." TNS, www.wis-tns.org/astronotes/astronote/2020-136.
3. ITelescope, www.itelescope.net/.

4. Kowal, C. T. "Absolute Magnitudes of Supernovae." The Astronomical Journal, vol. 73, 1968, doi:10.1086/110763.
5. Stevenson, David S. Extreme Explosions Supernovae, Hypernovae, Magnetars, and Other Unusual Cosmic Blasts. Springer, 2014.
6. Stetson, Peter B. "DAOPHOT - A Computer Program for Crowded-Field Stellar Photometry." Publications of the Astronomical Society of the Pacific, vol. 99, 1987, doi:10.1086/131977.
7. "New Mexico Skies - MPC H06 T11." Support, support. itelescope.net/support/solutions/articles/231903-telescope-11.
8. Fukugita, M., et al. "The Sloan Digital Sky Survey Photometric System." The Astronomical Journal, vol. 111, 1996, p. 1748., doi:10.1086/117915.
9. "Maxim DL - Astronomy & Scientific Imaging Solutions." Diffraction Limited, 17 Nov. 2021, diffractionlimited.com/product/maxim-dl/.
10. Chambers, Kenneth C., et al. "The Pan-STARRS1 surveys." arXiv preprint arXiv:1612.05560 (2016).

APPENDIX: Supplementary Material

Date, JDN	Telescope	Filters	Total Exposure
07/25/20 2459056.60	16-inch	g	(11 × 60s)
		r	(11 × 60s)
07/27/20 2459058.61	16-inch	g	(11 × 60s)
		r	(11 × 60s)
07/29/20 2459060.57	16-inch	V	(11 × 60s)
		R	(11 × 60s)
07/29/20 2459060.71	T11	g	(4 × 300s)
		r	(4 × 300s)
07/31/20 2459062.60	16-inch	g	(15 × 60s)
		r	(11 × 60s)
08/05/20 2459067.64	16-inch	g	(11 × 60s)
		r	(11 × 60s)

Table S1. Timing and exposure details for AT2020pni observations, done for both g and r filters.

Data Set	T_{vr}	C_{vr}	T_V	C_V
07/25 - 16 inch	0.9947	-0.2606	0.2546	24.5739
07/27 - 16 inch	0.7541	-0.0690	-0.0740	24.7433
07/29 - 16 inch	0.8396	-0.1095	0.1016	24.7484
07/29 - T11	1.3646	0.5378	0.7098	26.1626
07/31 - 16 inch	0.8221	-0.1519	0.0627	24.6843
08/05 - 16 inch	0.8875	-0.2509	0.1793	24.5464

Table S2. Calibration transformation coefficients for each set of data, to convert from instrumental magnitudes to apparent magnitudes.
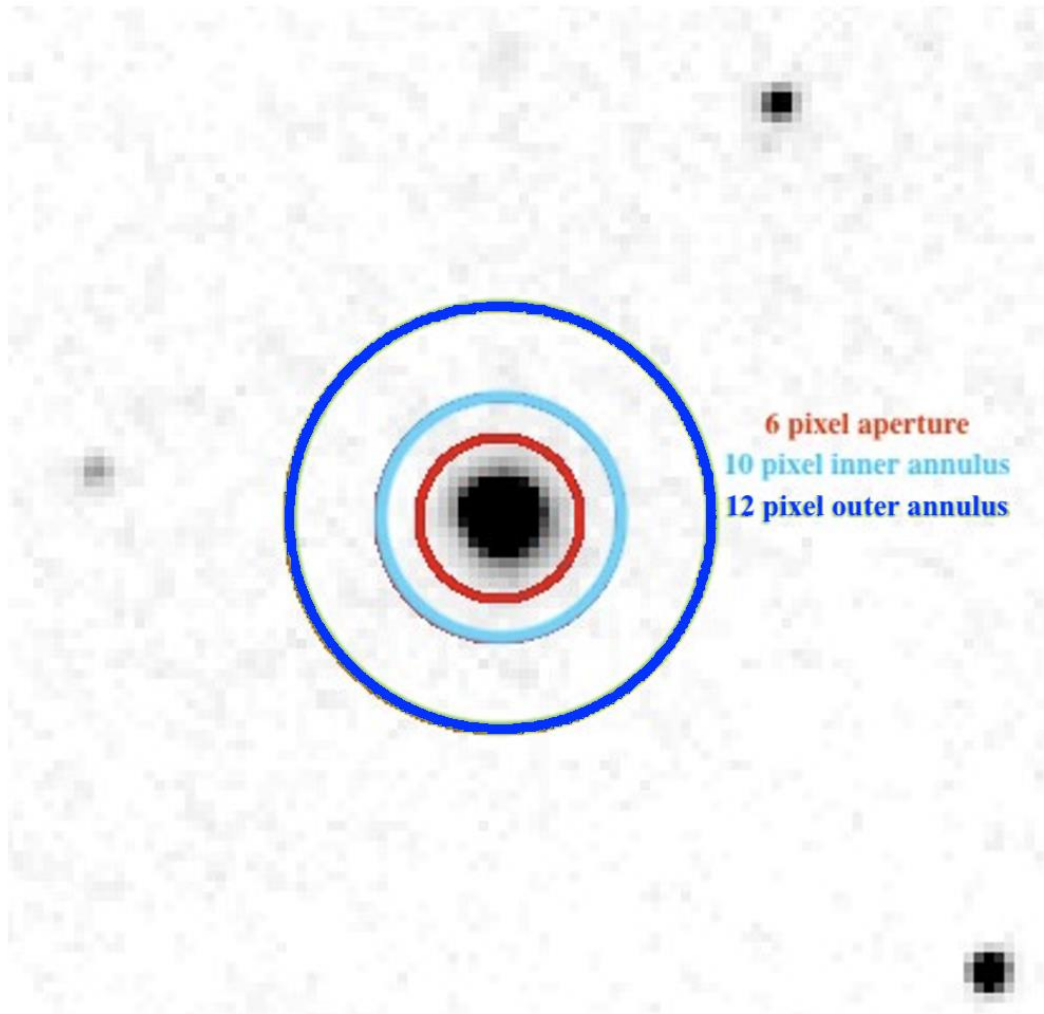
Figure S1. A Visual Illustration of a Circular Aperture and Annulus. A visualization of circular aperture and annulus used in our aperture photometry pipeline for standard stars. We utilized a 6-pixel-radius circular aperture around each star and an annulus with an inner radius of 10 pixels and an outer radius of 12 pixels.
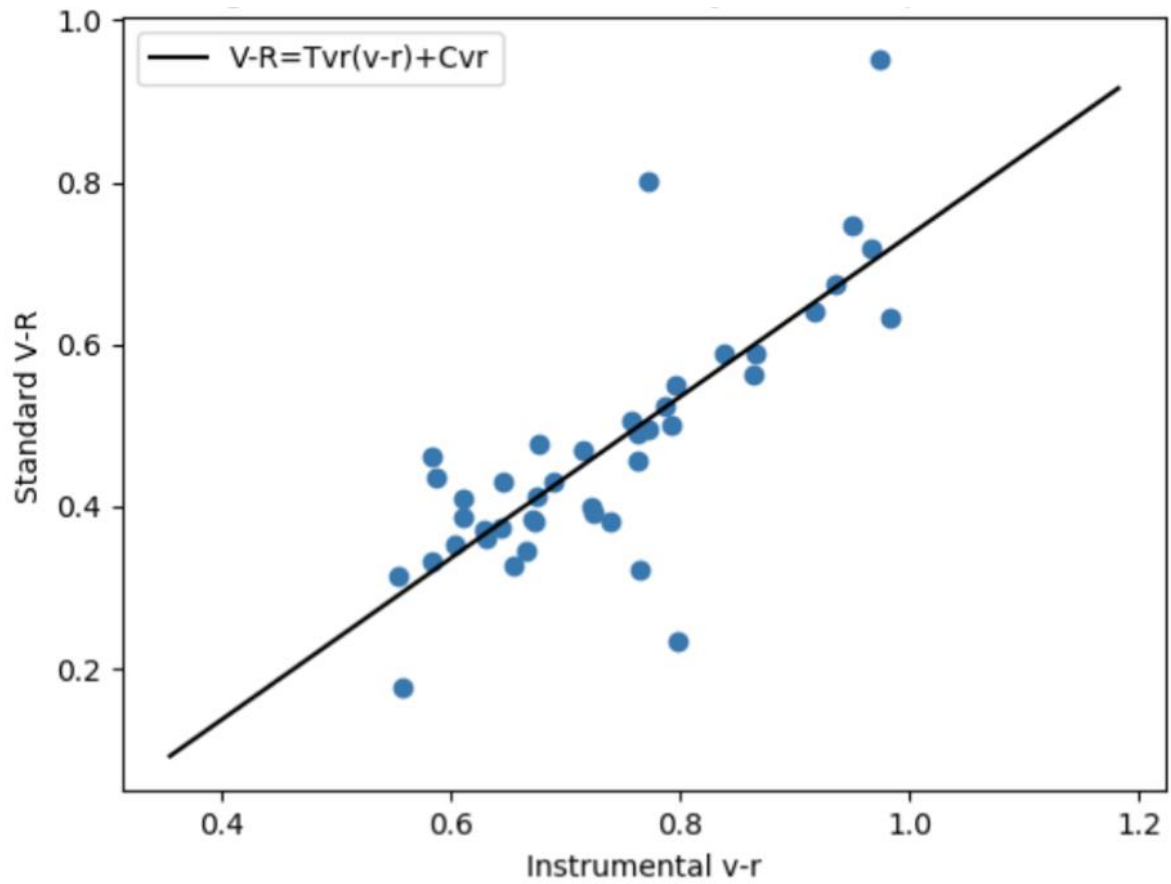
Figure S2. A Regression of The Standard and Instrumental Colors of The Standard Stars. An example linear regression of standard vs. instrumental colors of standard stars from our 16-inch LFOP telescope data on July 25th, 2020 is shown. The linear regression provides the transformation coefficients needed for the color-calibration of the supernova as shown in the BVR photometry equation provided.